Journal of Biomedical Optics

SPIEDigitalLibrary.org/jbo

Development of a new illumination procedure for photodynamic therapy of the abdominal cavity

Laurie Guyon
Jean Claude Lesage
Nacim Betrouni
Serge Mordon

SPIE

Development of a new illumination procedure for photodynamic therapy of the abdominal cavity

Laurie Guyon,[a,b] Jean Claude Lesage,[a] Nacim Betrouni,[a] and Serge Mordon[a,c]
[a]University Lille Nord de France, INSERM, U703, Lille University Hospital, Lille, France
[b]Lille University Hospital, Department of Gynaecology and Obstetrics, Lille, France
[c]GDR 3049, Médicaments Photoactivables—Photochimiothérapie (PHOTOMED)

Abstract. A homogeneous illumination of intra-abdominal organs is essential for successful photodynamic therapy of the abdominal cavity. Considering the current lack of outstanding light-delivery systems, a new illumination procedure was assessed. A rat model of peritoneal carcinomatosis was used. Four hours after intraperitoneal injection of hexaminolevulinate, a square illuminating panel connected to a 635-nm laser source was inserted vertically into the abdominal cavity. The abdominal incision was sutured and a pneumoperitoneum created prior to illumination. Light dosimetry was based on the calculation of the peritoneal surface by MRI. The rats were treated with a light dose of 20, 10, 5 or 2.5 J/cm^2 administered continuously with an irradiance of 7 mW/cm^2. The homogeneity of the cavity illumination was assessed by quantification of the photobleaching of the tumor lesions according to their localization and by scoring of that of the liver and of the bowel immediately after treatment. Photobleaching quantification for tumor lesions relied on the calculation of the fluorescence intensity ratio (after/before treatment) after recording of the lesions during blue-light laparoscopy and determination of their fluorescence intensity with Sigmascan Pro software. The procedure led to a homogeneous treatment of the abdominal cavity. No statistical difference was observed for the photobleaching values according to the localization of the lesions on the peritoneum ($p = 0.59$) and photobleaching of the liver and of the intestine was homogeneous. We conclude that this procedure can successfully treat the major sites involved in peritoneal carcinomatosis. [DOI: 10.1117/1.JBO.17.3.038001]

Keywords: photodynamic therapy; peritoneal carcinomatosis; light dosimetry; photobleaching; hexaminolevulinate.

Paper 11559 received Sep. 30, 2011; revised manuscript received Dec. 20, 2011; accepted for publication Jan. 11, 2012; published online Mar. 8, 2012.

1 Introduction

During their progression, gynecological and digestive cancers extend from the initial tumor site to other intra-abdominal organs. This metastatic evolution results in disseminated peritoneal lesions corresponding to what is called peritoneal carcinomatosis. The treatment of this condition usually relies on an extensive surgical resection of the tumor lesions along with chemotherapy. This treatment can be difficult to perform and comes with serious side effects; the prognosis of the disease remains poor.[1–5] Photodynamic therapy (PDT) is an investigational alternative to the conventional therapeutic strategies for the management of this often incurable disease.

The illumination of the different intra-abdominal organs, covered in potentially cancerous peritoneum, is one of the main challenges for PDT of the abdominal cavity. The abdominal cavity represents a complex association of volumes that need to be illuminated as completely as possible during PDT to eradicate all tumor implants.

Previous preclinical studies reported encouraging results of PDT of the peritoneal cavity, but the treatment prolonged the life of the animals without leading to their cure,[6–10] thus bringing into question the thoroughness of the treatment.

So far, different devices aiming to improve light distribution inside the abdomen have been described. They include flat optical fibers, refracting prisms, inflatable balloons, and rectangular blocks.[8,10–12] Lipid emulsions are also widely used to fill the abdominal cavity during treatment and act as a diffusing medium.[13–15] Their efficacy in terms of areas illuminated is scarcely discussed, despite its potential influence on the effectiveness and safety of PDT for peritoneal carcinomatosis.

In their clinical study, Sindelar et al.[15] treated patients by successively exposing the bowel and the mesentery to laser light using flat-cut optical fibers, then treating the rest of the cavity with a fiber placed in an inflatable balloon after filling the cavity with an Intralipid solution. They also performed real-time photometry to adapt their treatment. However, despite a long and aggressive technique, the results remained modest, with only six in 23 patients free of recurrence eight to 18 months after PDT.[15]

Lilge et al.[16] evaluated the distribution of light within the abdominal cavity of a murine model during PDT with optical fibers of different designs placed in different locations. Their photometry results showed that none of their procedure options led to a homogeneous illumination, a finding which was confirmed by the mapping of the residual tumor burden three days after PDT.[16]

Considering this lack of optimized illumination techniques, we developed a new illumination procedure for PDT of the abdominal cavity. This procedure was tested on Fischer 344 female rats with induced peritoneal carcinomatosis.

The photosensitizer used for the experiments was already documented. Hexaminolevulinate is already approved and its

Address all correspondence to: Serge Mordon, INSERM U703, Lille University Hospital, 152 rue du Drive, Yersin, 59120 LOOS, France, 59037. Tel: 33 320 446 708; Fax: 33 320 446 708; E-mail: serge.mordon@inserm.fr

0091-3286/2012/$25.00 © 2012 SPIE

use recognized for photodiagnosis of early bladder cancer;[17] it has also proved its efficacy for photodiagnosis of peritoneal carcinomatosis and for treatment of this disease on a limited peritoneal surface, including with continuous illumination with red light.[18,19] The other aspects of the procedure were newly developed.

An illuminating panel was inserted into the abdominal cavity. The cavity was continuously illuminated with a 635-nm laser light, with a fluence rate of 7 mW/cm^2 on the peritoneal surface. Light dosimetry was performed by calculation of the peritoneal surface by MRI. Illumination times were determined so as to reach fluences ranging from 2.5 to 20 J/cm^2, and treatments respectively lasted from five to 50 minutes. These parameters were chosen based on previous studies,[9,14,20] so as to guarantee that PDT would have an effect on tumor lesions and, consequently, that the illumination procedure could be properly assessed.

Indeed, instead of evaluating the efficacy of light distribution by complex *in vivo* dosimetry systems, we assessed light distribution by the response of different intra-abdominal structures to PDT. A homogeneous clinical response throughout the abdominal cavity was considered a more useful criterion to observe than homogeneous light measurements that might not necessarily be correlated with clinical response. It was previously shown in the same rat model that the importance of photobleaching correlated well with the response to PDT.[21] The same observation was made in PDT of the esophagus and of the skin.[22,23] Photobleaching of the lesions of the abdominal wall and of the diaphragm, as well as photobleaching of the liver and of the intestine immediately after treatment were thus used as the assessment criteria.

As described by Ascencio et al., photobleaching was assessed after recording of the lesions, before and after PDT, during a laparoscopy in blue-light mode.[21] The intensity of fluorescence of the lesions was calculated offline with a specific software. The photobleaching was then quantified by calculating the fluorescence intensity ratio after/before treatment (the "photobleaching value"). Where pathologic examinations might not have allowed an immediate postoperative evaluation or a complete exploration of the abdominal cavity, this technique allowed an early and exhaustive assessment of the homogeneity of the illumination within the abdominal cavity.

Once the performance of this illumination procedure is finally proven, its efficacy can be assessed in the long term.

2 Methods

2.1 *Animal Model*

NuTu-19 is a syngenic adenocarcinoma used to develop ovarian cancer in an immune-competent Fischer 344 rat model. It is a poorly differentiated adenocarcinoma originally derived from a female athymic mouse after injection of Fischer 344 ovarian surface epithelial cells that spontaneously underwent malignant transformation *in vitro*.[24]

NuTu19 cells were grown in Dulbecco's modified eagle medium (DMEM) (Gibco Life Technologies, Grand Island, NY, USA) supplemented with 10% heat-inactivated fetal bovine serum, 1% penicillin and 1% streptomycin. Culture plates were maintained in an incubator at 37°C in an atmosphere of 5% carbon dioxide.

Cells were harvested for injection when they were 80% to 100% confluent. For tumor cells' harvest and transplantation, cells were trypsinized (tripsyn-EDTA, Gibco Life Technologies), centrifuged at 1200 rpm for 10 min and re-suspended in phosphate-buffered saline (PBS) (Gibco Life Technologies). Cells were counted and their viability tested using the trypan blue exclusion test. Cells were considered for transplantation if the survival rate was at least 95%. The suspension volume was then adjusted to a concentration of $6 \cdot 10^6$ cells/mL.

Pathogen-free Fischer 344 female rats (Charles River Laboratories, L'Abresle, France) weighing 140 to 160 g were given intraperitoneal (IP) injection with $6 \cdot 10^6$ cells/mL from the NuTu19 cell line. The rats were housed throughout the whole experiment in a pathogen-free facility with commercial basal diet and water *ad libitum* and received proper care and maintenance.

They were monitored daily for signs of tumor growth. Animals showing an evident excessive tumor burden (abundant ascites, icterus, discolored eyes) were excluded from the experiments and were sacrificed.

The experiments were started between six and nine weeks after injection of the cells, because it has been shown that the injection of a 1-mL suspension containing 6.10^6 cells resulted in a reproducible disease progression *in vivo* and that peritoneal carcinomatosis was present from six weeks after the injection.

The protocol was approved by the animal use and ethics committee of Département Hospitalo-Universitaire de Recherche Expérimentale, Lille University, France.

2.2 *Photosensitizer*

Cristalline 5-aminolevulinic acid hexylester hydrochloride (HAL; Photocure ASA, Oslo, Norway) was stored in powder form and kept refrigerated. Samples were prepared immediately prior to use by dissolution of the powder in PBS, so as to obtain a concentration of 100 mg/mL, and were sheltered from light. Each animal received an IP injection of 100 mg/kg of HAL four hours prior to PDT.

2.3 *PDT Procedure*

The rats were anesthetized by IP injection of ketamine (50 mg/kg; Virbac, Carros, France) and Xylazine (50 mg/kg; Bayer Health Care, Puteau, France). They were placed in the supine position and a blue-light mode laparoscopy was performed for fluorescence analysis (cf. infra).

After photodiagnosis, the laparoscopy device was removed and a lower midline laparotomy was performed. A square illuminating panel (Lumitex, Strongsville, USA) was introduced vertically inside the abdominal cavity and was connected to a 635-nm laser source.

The panel was made of acrylic optical fibers which were abraded with a computer-controlled proprietary process known as UniGlo. The micro-abrasions disrupted the cladding to let the light out. By controlling the depth of the abrasions, the light was made uniform across the panel. The fibers were laminated directly onto a back reflector. The optical fibers extended from the panel in cable form and were bundled into a specifically manufactured highly polished brass ferrule. This ferrule was connected to the 635-nm diode laser (Dilas, Germany) [Fig. 1(a)]. The panel itself measured 2.54 by 2.54 by 0.1 cm and both sides illuminated homogeneously and continuously over time with a fluence rate of 45 mW/cm^2.

After the insertion of the panel, a 14-G catheter connected to the insufflation device used during the laparoscopy procedure

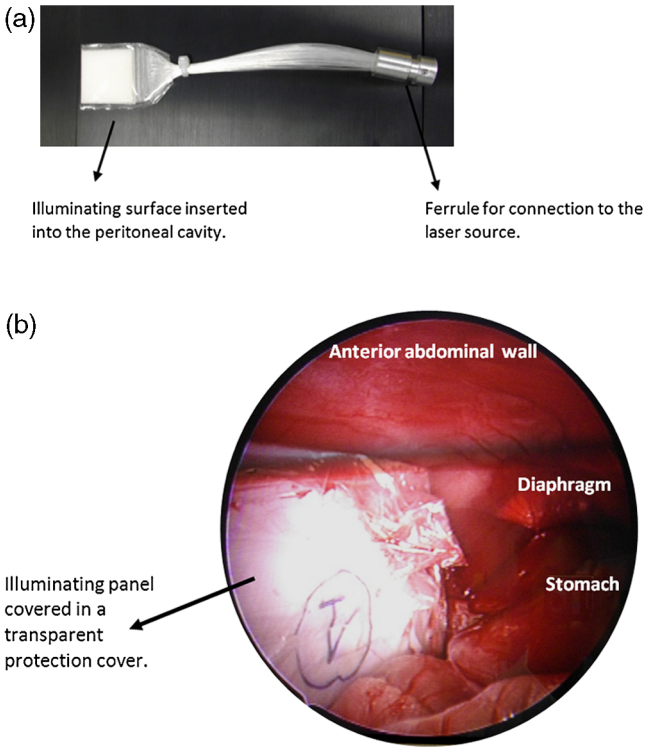

Fig. 1 Illuminating panel (Lumitex, Strongsville, USA). (a) Description of the illuminating panel. Illuminating surface inserted into the peritoneal cavity. Ferrule for connection to the laser source. (b) Illuminating panel placed vertically inside the abdominal cavity. The abdominal incision performed for its insertion was sutured and a 3-mmHg pneumoperitoneum was created. Illuminating panel covered in a transparent protection cover. Anterior abdominal wall. Diaphragm. Stomach.

was also inserted inside the abdominal cavity through the laparotomy incision. The laparotomy incision was hermetically sutured around the panel connector and the insufflation catheter and a 3-mmHg pneumoperitoneum was created [Fig. 1(b)].

The distance from the light source to the abdominal wall was maintained constant with the pneumoperitoneum. The insufflation catheter was maintained within the abdominal cavity throughout treatment and the pneumoperitoneum pressure was set at 3 mmHg on the insufflation device. Insufflation devices continuously monitor intra-abdominal pressure so that they immediately adapt their flow to pressure modifications in order to keep the flow constant. The abdominal incision created to insert the panel inside the abdominal cavity was sutured as hermetically as possible to avoid leaks. The fact that the incision was hermetically sutured was checked before starting the illumination by verifying that the intra-abdominal pressure was stable.

The rats were divided into four groups. Each group included three rats that were treated until a fluence of 20, 10, 5 or 2.5 J/cm^2 was reached with continuous illumination with a fluence rate of 7 mW/cm^2 on the peritoneal surface. After PDT and suturing of the laparotomy incision, a laparoscopy was performed in blue-light mode to assess the results of the treatment (cf. infra).

A fifth group of five rats underwent a sham procedure, receiving an injection of PBS (1 mL/100 g) instead of HAL four hours prior to light exposure. They were treated with a fluence of 20 J/cm^2. Three rats were sacrificed 48 hours after the procedure and two rats three weeks after, in search of early and late adverse events. After sacrifice, the rats underwent an autopsy and sampling of the intra-abdominal and thoracic organs for pathologic examination.

2.4 *Light Dosimetry*

The illumination time required to reach the desired fluence was calculated on the basis of an estimation of the peritoneal surface by MRI in a different set of rats.

2.5 *Preliminary Study*

Six to nine weeks after the injection of 6.10^6 NuTu19 cells, Fischer 344 female rats were weighed and anesthesized by IP injection of ketamine and xylazine. A 3-mmHg pneumoperitoneum was created by means of a 14-G catheter connected to the laparoscopy insufflation device (Karl Storz, Tuttlingen, Germany) and inserted into the abdominal cavity. At this step, the absence of bloody ascite was verified. It was confirmed by the absence of back-flow in the catheter before insufflation.

After obtaining the desired pneumoperitoneum, the catheter was removed and the opening was hermetically sutured. The rats were placed in the supine position in a 7-Tesla MRI machine (Biospec Bruker, Wissembourg, France). Ninety 1-mm-thick cross-sections covering the whole abdominal cavity were acquired in T1 sequence. TR/TE was 2033/9 ms; the axial field of view was 6 by 6 cm; and the axial resolution was 0.0234 cm per pixel.

The sections were entered in the Osirix software and the abdominal cavity, materialized by the pneumoperitoneum, was outlined on each section (Fig. 2). The abdominal cavity perimeters determined on each section were collected and the peritoneal surface exposed by the pneumoperitoneum was deducted from the addition of all the elementary surfaces calculated using the equation: perimeter x thickness of the section. The peritoneal surfaces were then correlated to the weight of the rats.

2.6 *Dosimetry During the PDT Procedure*

Before starting PDT, each rat was weighed if necessary after evacuation of ascites. Their peritoneal surface was calculated according to the results of the preliminary MRI study.

The fluence rate received by the peritoneal surfaces was determined by reporting the total power of the panel to this surface. It was calculated with the equation: FR $= P/$SP (where FR was the fluence rate in mW/cm^2 ; P was the power of both sides of the panel and equal to 581 mW; and SP was the peritoneal surface of the rat determined by the MRI study).

The illumination time was calculated using the equation: IT $= F/$FR (where IT was the illumination time in seconds; F was the desired fluence in mJ/cm^2; and FR was the fluence rate previously determined in mW/cm^2).

To check the coherence of the fluence rate calculated with the help of the MRI results, an *in vivo* photometry was performed on the rats undergoing PDT. An isotropic probe (Model IP, Medlight SA, Ecublens, Switzerland) was inserted into the abdominal cavity via the laparotomy incision and sutured to the middle of one of the sides of the rat. The extremity of the probe was placed 2 cm left of the midline and at mid-height of the abdominal cavity. The probe was connected to a hand-held optical power and energy meter (Model 841 PE, Newport, Irvine, CA, USA). Measurements were performed five minutes

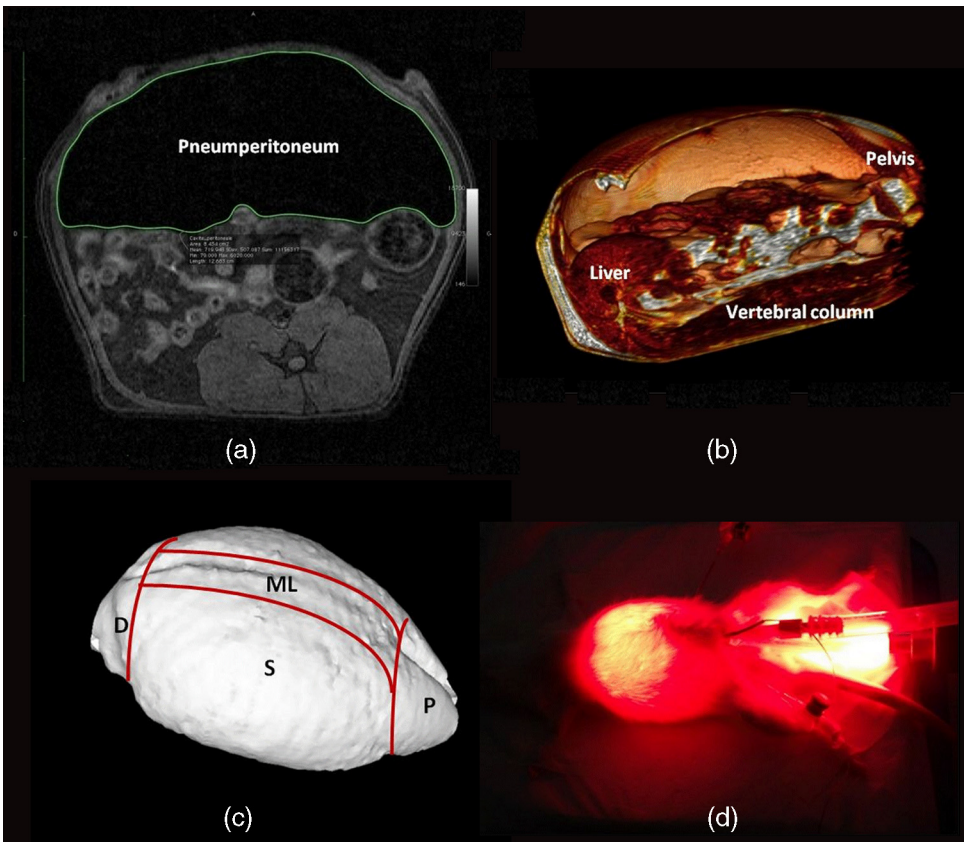

Fig. 2 Modeling of the peritoneal cavity with MRI after creation of a 3-mmHg pneumoperitoneum, rat laying on the back. (a) Example of peritoneal cavity outlining on an MRI abdominal cross-section with Osirix software. (b) Parasagittal section of a reconstruction of the peritoneal cavity volume based on MRI cross-sections. It shows the intra-abdominal surfaces exposed by the pneumoperitoneum. The upper part of the cavity is on the left; the midline is on top. (c) External view of the reconstructed peritoneal cavity volume. For the photobleaching analysis, different parietal areas were individualized: the diaphragm (D), the midline (ML), the sides (S) and the pelvis (P). (d) Peritoneal cavity revealed by panel illumination during PDT.

after the beginning of the treatment. A measure of the power at the contact of the panel was also taken before each *in vivo* measurement by placing an isotropic probe at its center. The fluence rate on the surface of the peritoneal membrane was calculated with the equation: $FR_{ps} = FR_{pc}(P_{ps}/P_{pc})$. FR_{ps} and P_{ps} were respectively the fluence rate and the power measured on the peritoneal membrane; FR_{pc} and P_{pc} were respectively the fluence rate and the power measured on the panel.

2.7 *Fluorescence Analysis*

The efficacy of the illumination procedure was assessed by the analysis of the photobleaching of the lesions. Fluorescence was monitored by laparoscopy before and after PDT as previously described.[21] A rigid 5-mm laparoscope (Karl Storz, Tuttlingen, Germany) was introduced through a trocar inserted in the lower midline. A 4-mmHg pneumoperitoneum was created and photodiagnosis of the peritoneal carcinomatosis was performed. The abdominal cavity was explored clockwise in white and in blue light mode (380–440 nm). The diaphragm, the midline and the sides (from the diaphragm to the upper part of the pelvis) were explored, as well as the liver and the bowel. A grip, inserted through a second trocar put on the laparotomy incision line, was used to help unroll the bowel and explore the liver.

In blue-light mode, tumor lesions were visualized as red fluorescent spots on a nonfluorescent peritoneum and were recorded on a digital recorder (DVR 30, Sony, Tokyo, Japan) connected to the laparoscope camera for photobleaching analysis.

Tumor lesions easily identifiable were recorded before and immediately after PDT. They were processed offline using Vpaint Sigma Scan Pro software (Systat version 5, San Jose, CA). The lesions were outlined and fluorescence intensities were measured at the center of each lesion as counts per pixel, in arbitrary units.

The photobleaching value corresponded to the ratio between the fluorescence intensity before illumination and the fluorescence intensity after illumination and was expressed as a percentage. Under 0.4 (i.e., when the residual fluorescence intensity was lower than 40% of the initial fluorescence intensity), the treatment was considered to be effective.[21] Photobleaching was analyzed according to the PDT protocol and to the localization of the lesions in the group of rats treated with a fluence of 10 J/cm^2.

The photobleaching of the liver and of the intestine was assessed by means of a score (Table 1). The fluorescence of both organs was subjectively evaluated before and just after PDT during the laparoscopy in blue-light mode. The intensity of fluorescence was categorized as no residual fluorescence (0), or low (1+), moderate (2+) or high (3+) intensity of fluorescence. Fluorescence was considered to be incomplete if it did not involve the entire organ and in case of incomplete fluorescence, the zone of highest intensity was taken into account. The subjective assessment of fluorescence had been correlated with

Table 1 Photobleaching scoring system for the liver and the bowel.

Residual fluorescence assessment	Scoring
No residual fluorescence	0
Low fluorescence	1+
Moderate fluorescence	2+
High incomplete fluorescence	3+

fluorescence-intensity measurements performed with the Sigmascan Pro software and validated by two different observers in a preliminary study (data not shown).

2.8 *Statistical Analysis*

The Kruskall Wallis's and Fischer's tests were used for the analysis of photobleaching results. The Spearman correlation coefficient was used for the analysis of the correlation between the weight of the rats and their peritoneal surface. A value of $p < 0.05$ was considered significant.

3 Results

3.1 *Dosimetry Results*

Eleven ascites-free rats underwent an MRI to determine their peritoneal surface. A correlation was found between the weight of the rats and the measure of their peritoneal surface ($p < 0.0001$, $R^2 = 0.943$; Fig. 3).

The peritoneal surface exposed by the 3-mmHg peritoneum was calculated for each rat using the following equation, determined with the curve describing the relationship between weight and peritoneal surface: $SP = 0.554 \times \text{weight} - 25.48$ (where SP was the peritoneal surface in cm^2).

Illumination times needed to reach different fluences in a rat weighing 200 g are reported in Table 2. For instance, for a rat weighing 200 g, the peritoneal surface was 85 cm^2, the irradiance was 6.8 mW/cm^2 and the rat was illuminated during 49 minutes to obtain a fluence of 20 J/cm^2.

The weight of the rats treated ranged between 185 and 210 g. Owing to the difference in their peritoneal surfaces, we calculated that if the same illumination time had been used for all of them, there would have been a difference of 4 J/cm^2 between the fluence of the lightest and that of the heaviest rat.

When compared with the measures obtained with the *in vivo* light dosimetry, the fluence rate on the peritoneal surface determined with the MRI results was coherent (Table 3).

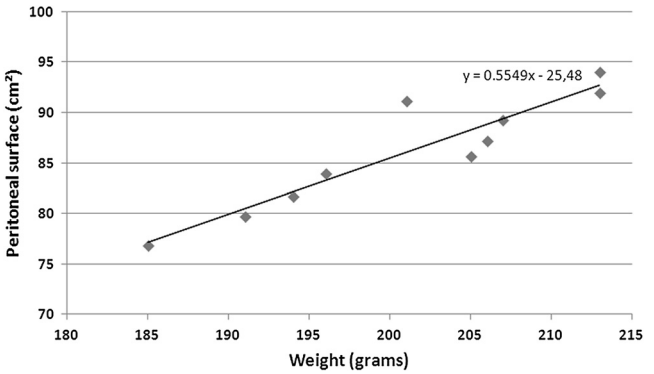

Fig. 3 Relation between peritoneal surface and weight as determined by MRI six to nine weeks after the injection of NuTu19 cells to Fischer 344 female rats.

Table 2 Treatment duration as calculated with the peritoneal surface determination with MRI, for a rat weighing 200 g.

Desired fluence	Treatment duration[a]
20 J/cm^2	49 minutes
10 J/cm^2	24 minutes 30 seconds
5 J/cm^2	12 minutes
2.5 J/cm^2	6 minutes

[a]Calculated with the equation: Duration = Fluence/((total Power of the panel/Peritoneal Surface) × 60).

3.2 *Assessment of the PDT Procedure*

3.2.1 *Outcome after the sham procedure*

The surgical procedure was easily performed and induced neither per- nor postoperative complications. All the rats that underwent this procedure were alive and well. In the three rats that were sacrificed 48 hours after the procedure, the autopsy and the pathologic examination were normal. The two rats followed up for three weeks after the procedure were finally sacrificed. No late adverse events related to the procedure were observed.

3.2.2 *Efficacy of the illumination procedure*

Among the 12 rats undergoing a PDT procedure, neither per- nor postoperative complications caused by the surgical procedure were recorded. Between 25 and 32 lesions were analyzed in each treatment group to assess the efficacy of the procedure. The fluorescence quantification showed that photobleaching significantly decreased (i.e., the photobleaching value increased) with the decrease of the light dose (Fig. 4).

Among the rats treated with a fluence of 10 J/cm^2, 31 lesions of the midline, 43 lesions of the diaphragm and 40 of the sides were analyzed. Photobleaching ranged between 0.06 and 0.47 for the diaphragm, 0.09 and 0.45 for the midline and 0.09 and 0.42 for the sides. There were fewer than two lesions with a photobleaching above 0.4 for each location. There was no statistical difference between the mean photobleaching value for the different locations of the lesions ($p = 0.59$; Fig 5).

During the laparoscopy in blue-light mode performed before PDT, a red fluorescence of the liver and of the intestine was noticed. Four hours after the IP injection of HAL, the fluorescence of the liver and of the intestine was homogeneous and assigned an intensity rating of 3+. After treatment, the liver and the intestine also experienced photobleaching, as reported in Table 4. Most of the rats had either no or only low-to-moderate partial residual fluorescence.

Table 3 Results of the *in vivo* photometry and comparison of fluence rate calculation with *in vivo* photometry and with MRI.

Power measured at the center of the panel, in μW	Power measured on one side of the rats, in μW	Fluence rate on the peritoneal surface, in mW/cm^2	
		Calculated with the in vivo power measurements	Calculated with the determination of the peritoneal surface with MRI[a]
1.61	0.358	10	7.2
[1.54–1.66]	[0.24–0.41]	[6,7–11.7]	[6.7–7.7]

[a]For each rat, an in vivo light-power measure was performed and the fluence rate was determined with the help of the MRI results for calculation of the treatment length.

4 Discussion

This article describes a new illumination procedure for PDT of the abdominal cavity. The procedure was both simple and quick to perform, as the illumination times reported in Table 2 show. In addition, the sham group demonstrated both the short- and long-term safety of the procedure itself.

The failure of previously published PDT procedures to attain a cure could be linked with a lack of homogeneity in the illumination of intra-abdominal surfaces. Mastering control of the light dose delivered to the rats is crucial to guaranteeing the reproducibility of the illumination. Some authors performing PDT of the abdominal cavity do not give precise dosimetry data and describe their light doses according to the abdominal quadrants to which light is administered.[14,25] However, this option precludes any verification of reproducibility and any generalization of the experiments to other species than that on which they were initially conducted.

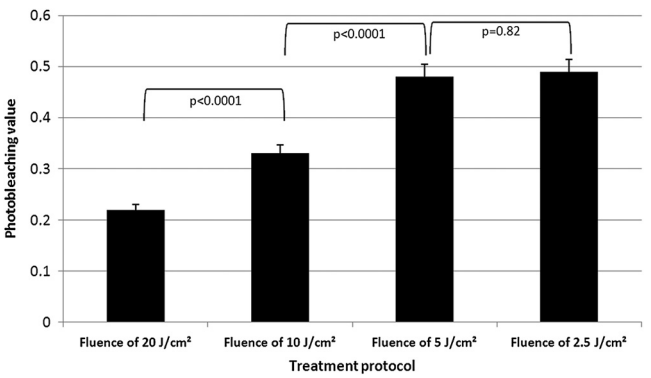

Fig. 4 Comparison of the mean photobleaching value according to the PDT protocol.

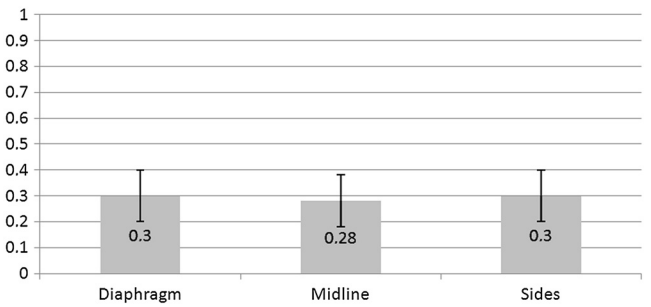

Fig. 5 Comparison of the mean photobleaching value according to the location of the lesions.

A second option is to calculate light doses according to peritoneal surface values and take the body surface as an estimation of the peritoneal surface.[7,13] This approach could not be used for our experiments because our procedure, which used a pneumoperitoneum to expose peritoneal surfaces, meant that only a part of the peritoneal surfaces were directly exposed to laser light. The surface exposed was thus much smaller than the complete parietal and visceral peritoneal surfaces, and the rats would have been at risk of a light overdose had the body surface been used as an estimate.

A third possibility is to perform *in vivo* dosimetry with photometry probes instead of calculating the light dose from the peritoneal surface.[8,26] With this aim in view, isotropic probes are more accurate than flat photodiodes.[27] However, it is difficult to obtain a reproducible dosimetry with isotropic probes, because the inframillimetric tip tends to get buried under fat or peritoneal folds, and its placement inside a catheter only partially prevents this drawback. Besides, the heterogeneity of the optical properties of the tissues leads to substantial variability of measurements (by a factor of at least 1.6).[27] Though our *in vivo* measures varied much in accordance with the previous considerations, they allowed us to confirm the coherence of the dosimetry deducted from the MRI study.

With MRI, a curve was obtained that allowed the determination of the peritoneal surface of each rat according to weight, and thus the calculation of light doses. Nevertheless, this curve is only valid in the described conditions and should be determined again in case of change of species.

We chose to determine the illumination time for each rat before treatment. Though the difference in peritoneal surfaces between the smallest and the biggest rats only led to a difference of 4 J/cm^2 between fluences, we wanted to eliminate as many causes of variability in treatment as possible.

We chose to assess the efficacy of the procedure with the quantification of the photobleaching of the lesions. Photobleaching was previously shown to reflect accurately the action of PDT on peritoneal carcinomatosis nodules, and in esophagus

Table 4 Photobleaching scoring results for the liver and the bowel.

Treatment protocol	Number of rats	Median liver photobleaching score	Median intestinal photobleaching score
Fluence of 10 J/cm^2	3	0.08	0.17
		[0–0.25]	[0–0.25]

or skin diseases, where immediate photobleaching also correlated with the response evaluated three months after treatment.[21–23]

After PDT was performed, instant visual assessment (and precise offline quantification) of the response of an important number of lesions and tissues was allowed. With a conventional strategy, this would require a pathological examination, which could be neither as early nor as exhaustive.[16]

For the liver and the bowel, the development of a specific scoring system was required to assess globally the action of light on these organs. The aim was to check that all major intra-abdominal areas had been properly exposed to light during the PDT procedure. The calculation of the photobleaching value would not have been accurate enough, as it requires the identification of precisely the same spot before and after PDT. In the case of the liver or of the bowel, no spot could be categorically recognized, especially as these organs' surfaces lack landmarks and the bowel could make spontaneous movements. Besides, photobleaching could be heterogeneous between their different zones, and the score took this specificity into account. The subjective assessment of fluorescence was reliable and easy to perform, but one should note that it was designed by observers who had the experience of photodiagnosis of peritoneal carcinomatosis. Experience enabled the creation of a mental scale of fluorescence intensities, as effective as objective measurements.

Photobleaching of peritoneal carcinomatosis lesions was precisely quantified in the literature and is associated with the importance of their necrosis after PDT. A threshold of 0.4 separates complete responders from nonresponders.[21]

In our study, the efficacy of the procedure increased in step with the light dose. Taking the threshold of 0.4 to distinguish photobleaching of the lesions that responded to PDT and that of lesions which did not, we concluded that treatments using a fluence of 20 J/cm^2 and 10 J/cm^2 were effective, whereas fluences of 5 J/cm^2 and below did not induce a satisfying response to the treatment. Besides, the majority of the lesions treated with 10 J/cm^2 had a photobleaching value under 0.4, which corresponds to a homogeneous response.

The fluence used in this experiment was chosen from the results obtained in previous studies.[9,14,20] The effective fluences may seem low compared to those often reported in the literature (frequently around 100 J/cm^2),[8,11,18,28] but several authors reported an increase in the efficiency of PDT with a decrease in the fluence rate.[29,30] The fluence rate used here was around 7 mW/cm^2 on the peritoneal surface, a value which corresponds to what other authors report as a very effective fluence rate.[29,31,32] Such low fluence rates imply a prolonged treatment in order to reach high fluences. However, their efficacy allows one to reduce the total light dose, and our illumination times remained short. The good results obtained with low fluence rates can by a mechanism of reoxygenation of the treatment site. Similarly, fractionated illumination during improves tumor response.[19] Three main mechanisms are thought to be involved in the enhancement of PDT response by light fractionation: reoxygenation of the treatment site, reperfusion injury and PpIX relocalization. Reoxygenation of the treatment site during the dark periods was proved to be essential. Oxygen depletion induced during the initial light period by temporary vascular constriction is reversed during the dark period. Curnow et al. have monitored the tissue oxygen pressure during fractionated and continuous illumination.[33] They observed a rapid decline in oxygen near the treatment site after beginning illumination and a partial recovery in oxygen during the dark period, whereas the decline in oxygen was irreversible during continuous illumination. In the case of fractionated light dose, this oxygen depletion during illumination is induced by temporary vascular constriction that is reversed during the dark period. Protoporphyrin IX relocalization could also enhance effects of light fractionation. It could be the result of local diffusion or reperfusion of plasma-bound PpIX.[34] The same processes could be involved in PDT with low fluence rates, due to a slower consumption of oxygen and thus of PpIX, allowing these components, which are essential to PDT, to regularly reach the treatment site.

Along with the illumination parameters chosen, the efficacy of our illumination procedure in terms of areas exposed to laser light could also have been questioned. Indeed, no manipulation other than a pneumoperitomeum was made to expose the different peritoneal surfaces.

The procedure proved very effective at treating lesions localized on the diaphragm, the midline and the sides (including the upper part of the pelvis). It could also induce an almost complete photobleaching of the bowel and of the liver, despite the absence of a specific procedure for the illumination of these organs. This may be due to the depth of penetration of red light inside the tissues and also to spontaneous movements of the intestinal tube, with the implication that tumor lesions of the bowel and the liver could also be treated.[35]

This study did not include the evaluation of the paracolic gutters and of the retrohepatic space, because in our tumor model, there were hardly any lesions in those locations unless the peritoneal carcinomatosis was very advanced. A long-term follow-up should allow confirmation of their treatment by proving the cure of the animals or, if applicable, by listing the preferential areas of recurrence.

The size of the device and the surgical procedure will require adaptations in order to be able to fit the peritoneal cavity of humans. The INSERM U703 laboratory is currently developing textile light diffusers of large surface that might help to illuminate the abdominal areas that are the most difficult to reach with a more rigid system—for example, the retrohepatic space and the paracolic gutters.[36]

A reliable calculation of the peritoneal surface that will be illuminated must also be determined, but this experiment shows that a standardized and reproducible treatment of peritoneal carcinomatosis with PDT is indeed possible.

5 Conclusion

Our illumination procedure was easy to perform and successful in treating the main localizations of peritoneal carcinomatosis. The estimation of the peritoneal surface by MRI proved to be possible and allowed for a reliable determination of the light dose administered, a step which lead to a reproducible photobleaching of all areas examined.

Acknowledgments

The authors are grateful to Karl Storz, Germany, Lumitex, USA, and Photocure ASA, Norway, for generously providing us with the laparoscopy equipment, the light panels and the photosensitizer respectively. The authors wish to thank Florent Auger and Nicolas Durieux for performing MRI and Joël Cliquenois, Arnold Dive and Michel Pottier for their technical support.

References

1. Surveillance, Epidemiology, and End Results (SEER) Program, "SEER*Stat Database: Populations –total US (1969-2007)," *National Cancer Institute, Division of Cancer Control and Population Sciences, Surveillance Research Program, Cancer Statistics Branch, Bethestda, MD (released April* **2011**, based on the November 2010 submission).
2. D. S. Chi et al., "Improved optimal cytoreduction rates for stages IIIC and IV epithelial ovarian, fallopian tube and primary peritoneal cancer: a change in surgical approach," *Gynecol. Oncol.* **94**(3), 650–654 (2004).
3. D. S. Chi et al., "The incidence of major complications after the performance of extensive upper abdominal surgical procedures during primary cytoreduction of advanced ovarian, tubal and peritoneal carcinomas," *Gynecol. Oncol.* **119**(1), 38–42 (2010).
4. J. Miller and A. Proletto, "The place of bowel resection in initial debulking surgery for advanced ovarian cancer," *Aust. NZ Obstet. J. Gynaecol.* **42**(5), 535–537 (2002).
5. D. Elias et al., "Peritoneal carcinomatosis treatment with curative intent: the Institut Gustave-Roussy experience," *Eur. J. Surg. Oncol.* **23**(4), 317–321 (1997).
6. W. Zhong et al., "In vivo high-resolution fluorescence microendoscopy for ovarian cancer detection and treatment monitoring," *Br. J. Cancer* **101**, 2015–2022 (2009).
7. A. L. Major et al., "Intraperitoneal photodynamic therapy in the Fischer 344 rat using 5-aminolevulinic acid and violet laser light : a toxicity study," *J. Photochem. Photobiol. B* **66**, 107–114 (2002).
8. R. B. Veenhuizen et al., "Intraperitoneal photodynamic therapy: comparison of red and green light distribution and toxicity," *Photochem. Photobiol.* **66**, 389–395 (1997).
9. S. Coutier et al., "Effect of irradiation fluence rate on the efficacy of photodynamic therapy and tumor oxygenation in meta-tetra (hydoxyphenyl) chlorine (mTPHC)-sensitized HT29 xenografts in nude mice," *Rad. Res.* **158**, 339–345 (2002).
10. R. B. Veenhuizen et al., "Intraperitoneal photodynamic therapy of the rat CC531 adenocarcinoma," *Br. J. Cancer* **73**, 1387–1392 (1996).
11. K. Song et al., "Intraperitoneal photodynamic therapy for an ovarian cancer ascite model in Fischer 344 rat using hematoporphyrin monomethyl ether," *Cancer Sci.* **98**, 1959–1964 (2007).
12. Z. Tochner et al., "Photodynamic therapy of the canine peritoneum: normal tissue response to intraperitoneal and intravenous photofrin followed by 630 nm light," *Lasers Surg. Med.* **11**, 158–164 (1991).
13. R. R. Perry et al., "Intravenous vs intraperitoneal sensitizer: complications for intraperitoneal photodynamic therapy," *Photochem. Photobiol.* **53**, 335–340 (1991).
14. K. L. Molpus et al., "Intraperitoneal photodynamic therapy of human epithelial ovarian carcinomatosis in a xenograft murine model," *Cancer Res.* **56**(5), 1075–1082 (1996).
15. W. F. Sindelar et al., "Technique of photodynamic therapy for disseminated intraperitoneal malignant neoplasms: phase I study," *Arch. Surg.* **126**, 318–324 (1991).
16. L. Lilge et al., "Light dosimetry for intraperitoneal photodynamic therapy in a murine xenograft model of human epithelial ovarian carcinoma," *Photochem. Photobiol.* **68**, 281–288 (1998).
17. P. U. Malmström et al., "Role of hexaminolevulinate-guided fluorescence cystoscopy in bladder cancer: critical analysis of the latest data and European guidance," *Scand. J. Urol. Nephrol, Early online* **16**, (Nov. 2011), [Epub ahead of print].
18. J. P. Estevez et al., "Continuous or fractionated photodynamic therapy? Comparison of three PDT schemes for ovarian peritoneal micrometastasis treatment in a rat model," *Photodiagn. Photodyn. Ther.* **7**, 251–257 (2010).
19. M. Ascencio et al., "Comparison of contunuous and fractionated illumination during hexaminolevulinate-photodynamic therapy," *Photodiagn. Photodyn. Ther.* **5**, 210–216 (2008).
20. M. G. Del Carmen et al., "Synergism of epidermal growth factor receptor-targeted immunotherapy with photodynamic treatment of ovarian cancer in vivo," *J. Natl. Cancer Inst.* **97**(20), 1516–1524 (2005).
21. M. Ascencio et al., "Protoporphyrin photobleaching is a useful tool to predict the response of rat ovarian cancer following hexaminolevulinate photodynamic therapy," *Lasers Surg. Med.* **40**, 332–340 (2008).
22. I. A. Boere et al., "Monitoring in situ dosimetry and protoporphyrin IX fluorescence photobleaching in the normal rat esophagus during 5-aminolevulinic acid photodynamic therapy," *Photochem. Photobiol.* **78**, 271–277 (2003).
23. J. S. Tyrrell, S. M. Campbell, and A. Curnow, "The relationship between protoporphyrin IX photobleaching during real-time dermatological methyl-aminolevulinate photodynamic therapy (MAL-PDT) and subsequent clinical outcome," *Lasers Surg. Med.* **42**, 613–619 (2010).
24. G. S. Rose et al., "Development and characterization of a clinically useful animal model of epithelial ovarian cancer in the Fischer 344 rat," *Am. J. Obstet. Gynecol.* **175**, 593–599 (1996).
25. Z. Tochner et al., "Treatment of murine intraperitoneal ovarian ascetic tumor with hematoporphyrin derivative and laser light," *Cancer Res.* **45**, 2983–2987 (1985), [Epub ahead of print].
26. G. M. Griffin et al., "Preclinical evaluation of Motexafin Lutetium-mediated intraperitoneal photodynamic therapy in a canine model," *Clin. Cancer Res.* **7**, 374–381 (2001), [Epub ahead of print].
27. T. G. Vulcan et al., "Comparison between isotropic and nonisotropic dosimetry systems during intraperitoneal photodynamic therapy," *Lasers Surg. Med.* **26**, 292–301 (2000).
28. T. M. Sitnik and B. W. Henderson, "The effect of fluence rate on tumor and normal tissue responses to photodynamic therapy," *Photochem. Photobiol.* **67**, 462–466 (1998).
29. B. W. Henderson, T. M. Busch, and J. W. Snyder, "Fluence rate as a modulator of PDT mechanisms," *Lasers Surg. Med.* **38**, 489–493 (2006).
30. M. S. Mathews et al., "The effects of ultra low fluence rate single and repetitive photodynamic therapy on glioma spheroids," *Lasers Surg. Med.* **41**, 578–584 (2009).
31. J. C. Finlay et al., "Porphyrin bleaching and PDT-induced spectral changes are irradiance dependent in ALA-sensitized normal rat skin in vivo," *Photochem. Photobiol.* **73**, 54–63 (2001).
32. D. J. Robinson et al., "Fluorescence photobleaching of ALA-induced protoporphyrin IX during photodynamic therapy of normal hairless mouse skin: the effect of light dose and irradiance and the resulting biological effect," *Photochem. Photobiol.* **67**, 140–149 (1998).
33. A. Curnow, J. C. Haller, and S. G. Bown, "Oxygen monitoring during 5-aminolaevulinic acid induced photodynamic therapy in normal rat colon: comparison of continuous and fractionated light regimes," *J. Photochem. Photobiol. B* **58**, 149–155 (2000).
34. W. Dietel et al., "5-Aminolaevulinic acid (ALA) induced formation of different fluorescent porphyrins: a study of the biosynthesis of porphyrins by bacteria of the human digestive tract," *J. Photochem. Photobiol. B* **86**, 77–86 (1997).
35. J. Eichler, J. Knof, and H. Lenz, "Measurements on the depth of penetration of light (0.35–1.0 μm) in tissue," *Rad. Environm. Biophys.* **14**, 239–242 (1977).
36. S. Mordon et al., "Innovative engineering design of a textile light diffuser for photodynamic therapy," *Photodiagn. Photodyn. Ther.* **8**, 142–143 (2011).